Anion Effect on the Structural Diversity of 1-D and 2-D Zinc(II) Coordination Polymers with a Flexible Fluorinated Bis(imidazole) Ligand

Feng Tian, Hong-Dan Wang, Ming-Yang He, Qun Chen, and Sheng-Chun Chen

Key Laboratory of Fine Petro-chemical Technology, Changzhou University, Changzhou 213164, P. R. China

Reprint requests to Dr. S.-C. Chen and Prof. M.-Y. He. Fax: +8651986330251.
E-mail: cscczu@yahoo.com (S.-C. Chen), hmy@cczu.edu.cn (M.-Y. He)

Z. Naturforsch. **2014**, *69b*, 878 – 884 / DOI: 10.5560/ZNB.2014-4123
Received June 22, 2014

Reactions of a flexible fluorinated ligand, 2,3,5,6-tetrafluoro-1,4-bis(imidazol-1-yl-methyl)benzene (Fbix), with ZnX_2 ($X = OAc^-$ or NO_3^-) lead to the formation of the two new Zn^{II} coordination polymers $[Zn(Fbix)(OAc)_2]_n$ (**1**) and $\{[Zn_2(Fbix)_3(NO_3)_2](NO_3)_2(H_2O)_3\}_n$ (**2**), which have been characterized by elemental analysis, IR spectroscopy, and single-crystal X-ray diffraction. Although the Zn^{II} centers of both **1** and **2** are in a similar tetrahedral coordination geometry, each Zn^{II} ion in **1** is surrounded by two Fbix spacers and two terminal OAc^- anions to form a highly undulated chain, whereas each Zn^{II} ion in **2** is embraced by three Fbix ligands and one NO_3^- anion to result in a two-dimensional cationic network. Since **1** and **2** are synthesized under the same conditions, the structural differences between them are attributable to the difference of the counterions. The solid-state properties such as thermal stability and luminescence of **1** and **2** have also been studied briefly.

Key words: Fluorinated Bis(imidazole) Ligand, Zn^{II} Coordination Polymer, Anion Effect, Crystal Structure, Luminescence Properties

Introduction

Over the past decade, the design and construction of coordination polymers and related metal-organic frameworks have witnessed tremendous growth owing to their intriguing structures and potential applications as functional materials [1 – 4]. Indeed, the properties of materials are determined by their structures. However, the formation of such coordination structures is highly sensitive to many factors such as the coordination preference of metal ions [5], the nature of organic ligands [6], counterions [7], solvents [8], and even the reaction temperature [9]. In particular, the role of the counterions in self-assembly processes has emerged as an increasingly important theme in recent studies [10 – 12]. Therefore, the understanding of the connection between complex structures and the factors affecting the framework formation is of great importance for the rational design of crystalline materials, but this still seems to be a long-term challenge.

Bis(imidazole) derivatives, as an important family of *N*-heterocyclic bridging ligands, have attracted great interest. Among them, 1,4-bis(imidazol-1-yl-methyl) benzene (bix) and related spacers have shown a certain ability to bridge different transition metal ions to give a variety of coordination motifs including discrete metallomacrocyclic molecules, and one-, two- and three-dimensional (1-D, 2-D, and 3-D) network architectures [13 – 15]. For example, Robson and coworkers reported a 2-D polyrotaxane structure of composition $[Zn(bix)_2(NO_3)_2]\cdot 2.5H_2O$ [14]. Ciani's group presented the assembly of bix with Zn^{II} sulfate, yielding a new coordination framework $[Zn_2(bix)_3(SO_4)_2]$ containing an unprecedented parallel (1-D → 2-D) interlacing array [15]. However, few examples have been synthesized to date, and little is known of the structural chemistry of fluorinated derivatives of bis(imidazole) or bis(triazole) ligands in inorganic-organic hybrid materials [16 – 19]. In this regard, Shreeve and coworkers have reported a series of Cd^{II}, Co^{II} and Ag^{I}

complexes constructed from 2,3,5,6-tetrafluoro-1,4-bis(imidazol-1-yl-methyl)benzene (Fbix, fluorinated analog of bix), exhibiting diverse structures from 1-D to 3-D [18]. Recently, we have illustrated the solvent-regulated conformational isomerism of Fbix on the construction of 1-D and 2-D Cu^{II} coordination polymers [20]. As a continuation of our research, herein, we wish to report two anion-controlled coordination polymers $[Zn(Fbix)(OAc)_2]_n$ (**1**) and $\{[Zn_2(Fbix)_3(NO_3)_2](NO_3)_2(H_2O)_3\}_n$ (**2**), which were assembled from Fbix with Zn^{II} salts with the anions OAc^- and NO_3^-, respectively. In addition, the spectroscopic, thermal, and luminescence properties of both complexes were also investigated as described below.

Results and Discussion

Synthesis and general characterization

The ligand Fbix is very soluble in common organic solvents (such as CH_2Cl_2, $CHCl_3$, CH_3OH, and CH_3CN), so that crystallization of its complexes with metal salts occurs readily. Complexes **1** and **2** were prepared by the reaction of Fbix with $Zn(OAc)_2{\cdot}2H_2O$ or $Zn(NO_3)_2{\cdot}6H_2O$ in methanol solution at room temperature. It should be pointed out that, in such specific reactions, the products do not depend on the ligand-to-metal ratio. However, increasing the ligand-to-metal ratio resulted in somewhat better crystal quality. We have not obtained any complexes suitable for X-ray analysis under the same conditions while using other Zn^{II} salts, such as $ZnCl_2$, $Zn(ClO_4)_2{\cdot}6H_2O$ and $Zn(BF_4){\cdot}6H_2O$. The IR spectra of the two complexes show absorption bands resulting from the skeletal vibrations of the aromatic rings in the 1600 – 1400 cm^{-1} region. Bands with medium intensity at 3145 cm^{-1} for **1** and 3121 cm^{-1} for **2** are associated with Ar–H stretching. For **1**, the characteristic bands of the acetate anions appear at 1618 cm^{-1} for $\nu_{as(C-O)}$, 1398 cm^{-1} for $\nu_{sym(C-O)}$ and 746 cm^{-1} for $\delta_{(O-C-O)}$. The value $\Delta(\nu_{as}-\nu_{sym})$ indicates that the acetate anion coordinates to the Zn^{II} center in a monodentate mode. For **2**, the broad band centered at *ca.* 3446 cm^{-1} indicates the O–H stretching of the water molecules. The absorption band at 1384 cm^{-1} is consistent with the existence of the NO_3^- anion in **2**.

*Structural description of complexes **1** and **2***

*$[Zn(Fbix)(OAc)_2]_n$ (**1**)*

X-Ray diffraction analysis reveals that complex **1** crystallizes in the monoclinic space group $C2/c$ and

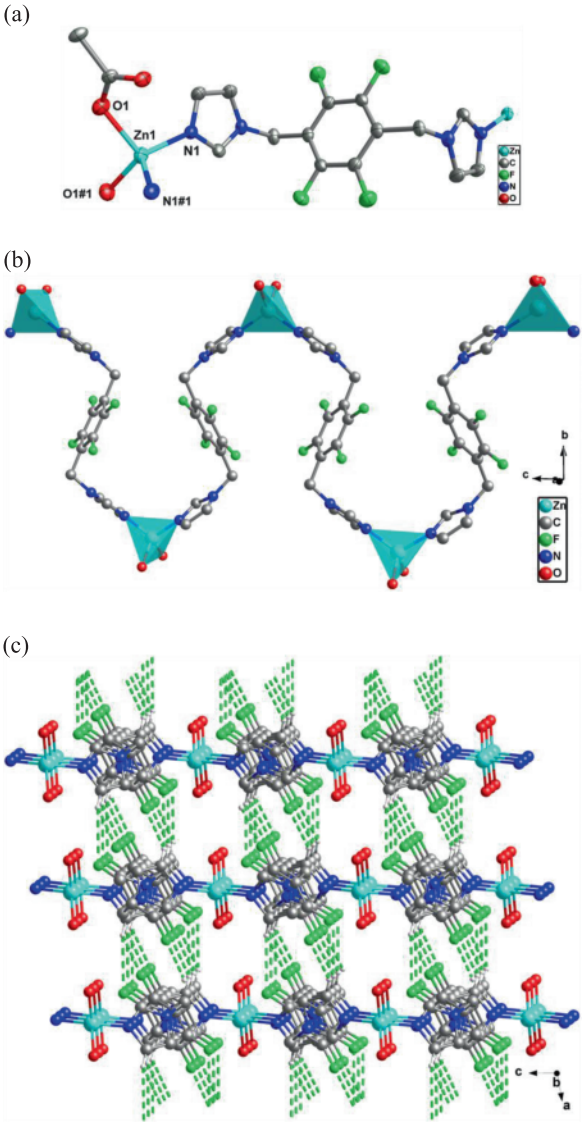

Fig. 1 (color online). Views of: (a) the coordination environment of the Zn^{II} center in **1** (symmetry code: #1, $-x+1$, y, $-z+1/2$), (b) the polymeric chain of **1** and (c) the 3-D supramolecular architecture (C–H···F hydrogen bonds are shown as dashed lines, irrelevant hydrogen atoms are omitted for clarity).

Table 1. Hydrogen bond geometries in the crystal structures of **1** and **2**.

Complex	D–H···A	H···A (Å)	D···A (Å)	D–H···A (deg)	Symmetry code
1	C3–H3···O2	2.50	3.107(3)	123	$-x+1, y, -z+1/2$
	C4–H4A···O1	2.60	3.255(3)	125	$-x+1, -y+1, -z+1$
	C1–H1···F1	2.78	3.520(1)	137	$-x+1/2, -y+1/2, -z+1$
	C1–H1···F2	2.70	3.534(4)	149	$-x+1/2, -y+1/2, -z+1$
2	O8–H8A···O9	2.23	2.950(2)	141	$x+1, y, z$
	C2–H2···O4	2.38	3.270(8)	160	$-x+1, -y+1, -z+1$
	C16–H16···O5	2.58	3.463(1)	159	$-x+1, -y+1, -z$
	O8–H8B···F2	2.51	3.251(9)	146	$x+1, y, z$
	C3–H3···F6	2.75	3.477(5)	136	$-x+1, -y+1, -z$
	C11–H11A···F5	2.76	3.507(7)	134	$x-1, y, z$
	C18–H18B···F2	2.97	3.868(8)	155	$x+1, y, z$
	O7–H7A···O6	1.75	2.590(2)	171	
	O9–H9A···O5	2.36	3.030(1)	136	
	O9–H9A···O6	2.18	3.011(1)	164	
	C3–H3···O5	2.41	2.231(1)	148	
	C17–H17···O4	2.46	3.198(8)	136	

has a neutral chain structure. The asymmetric unit of **1** contains one Zn^{II} ion, one Fbix ligand and two OAc^- anions. As shown in Fig. 1a, the tetrahedral coordination sphere of the Zn^{II} center is provided by two nitrogen donors from two Fbix ligands with the Zn–N distance of 2.004(2) Å, and two oxygen atoms from two OAc^- anions with a Zn–O distance of 1.962(2) Å. The Fbix ligand adopts an *anti* configuration, and the benzene ring makes a dihedral angle of 80.21(8)° with the imidazole ring, while two terminal imidazole rings within each ligand are essentially parallel. Thus, the Fbix ligand functions as a bidentate bridging spacer, using two terminal imidazole nitrogen atoms to link two Zn^{II} ions and form a highly undulated chain along the [001] direction (Fig. 1b), within which the successive Zn···Zn separations are 13.449(3) and 13.717(3) Å. In the packing arrangement, these polymeric chains are further linked by weak C–H···F hydrogen bonds (Table 1) between imidazole ring carbon atoms and fluorine atoms, leading to a 3-D supramolecular architecture (Fig. 1c).

*{[Zn_2(Fbix)$_3$(NO_3)$_2$](NO_3)$_2$(H_2O)$_3$}$_n$ (**2**)*

When the metal salt $Zn(OAc)_2{\cdot}2H_2O$ was replaced by $Zn(NO_3)_2{\cdot}6H_2O$, colorless block-shaped single crystals of **2** suitable for X-ray structure analysis were obtained by a similar synthetic procedure as that for **1**. The structure determination shows that complex **2** crystallizes in the triclinic space group $P\bar{1}$ and displays a cationic layered structure. The asymmetric unit consists of three components: one cationic unit $[Zn(Fbix)_{1.5}(NO_3)]^+$, one NO_3^- anion, and one and a half of lattice water molecules. As shown in Fig. 2a, each Zn^{II} ion adopts a distorted tetrahedral coordination geometry and is coordinated by three nitrogen donors from three different Fbix ligands with the Zn–N distances varying from 1.987(2) to 2.001(2) Å, and one oxygen atom from a monodentate nitrate anion with the Zn–O distance of 2.009(2) Å. Similar to **1**, the Fbix ligand in **2** adopts the *anti* conformation to avoid the steric hindrance, and the two imidazole rings are parallel to each other within each Fbix, where the dihedral angles between benzene rings and the imidazole rings are 75.0(1), 79.2(1) and 88.8(1)°. In this structure, three kinds of crystallographically independent Fbix ligands serve as 2-connected spacers to link adjacent Zn^{II} ions with the Zn···Zn distances of 12.951(1), 13.612(1) and 15.103(1) Å. Convercely, each Zn^{II} ion in **2** is linked to three Fbix ligands, resulting in a 2-D (6,3) brick-wall network parallel to the *bc* plane (Fig. 2b). The rhombic tiles are of approximate parallelogram dimensions 27.781(2) × 13.612(1) $Å^2$, with the NO_3^- counterions and guest water molecules being included in the voids. These layers are packed in the *ABCABC* sequence along the *c* direction (Fig. 2c), with *A*, *B* and *C* being related by the *a* glide plane. These layers are further linked by intermolecular C–H···O interactions (C16–H16A···O4, C9–H9A···O4, C10–H10A···O5 and C17–H17A···O5, see Table 1 for details) between imidazole rings and the uncoordinated

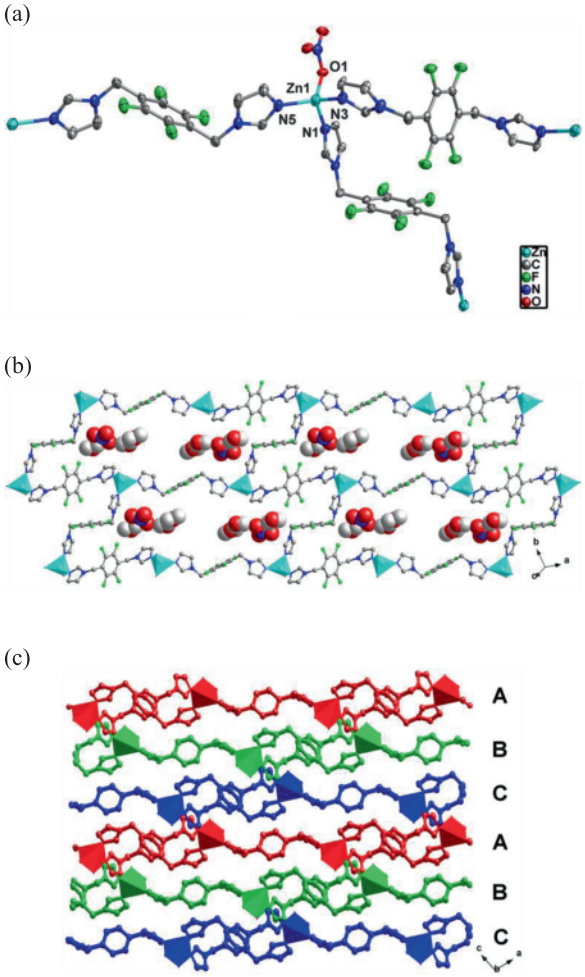

Fig. 2 (color online). Views of: (a) the coordination environment of the Zn^{II} center in **2**, (b) the layer structure extending along the *bc* plane and (c) the packing mode of parallel layers of **2** along the *c* direction.

NO_3^- anions, leading to the final 3-D supramolecular network.

Thermal stability

To investigate the thermal stability of complexes **1** and **2**, thermogravimetric analyses (TGA) were carried out from room temperature to 800 °C. The corresponding curves are depicted in Fig. 3. For **1**, the first weight loss of 24.1 % may tentatively correspond to the loss of two acetic acid molecules (calculated 23.9 %) in the temperature range of 40 – 180 °C. Then, pyrolysis of organic components is observed upon heating to *ca.* 250 °C. Further heating to 800 °C reveals continuous weight losses, and the residual holds a weight of 16.6 % of the total sample. In the case of **2**, the TG curve shows that the first weight loss of 4.3 % occurring from 80 °C to *ca.* 160 °C corresponds to the release of lattice water molecules (calculated 3.9 %). The decomposition of the residuary coordination framework occurs from *ca.* 280 °C and ends at 600 °C. Upon further heating to 800 °C, no weight loss is found, and the final solid holds a weight of 12.1 % of the total sample, which is close to that of ZnO (calculated 11.9 %).

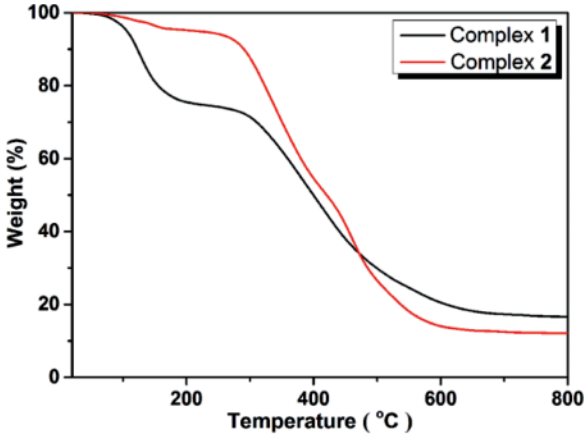

Fig. 3 (color online). TGA curves of complexes **1** and **2**.

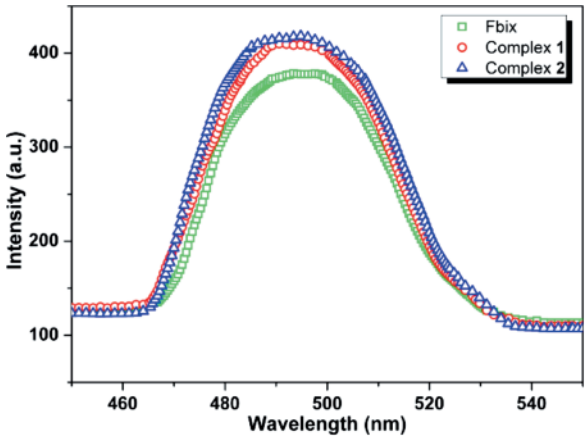

Fig. 4 (color online). Solid-state fluorescence emission spectra of the ligand Fbix, and of complexes **1** and **2**.

Photoluminescence properties

Taking into account the excellent luminescence properties of many other d^{10} Zn^{II} complexes, the luminescence behavior of the ligand Fbix and complexes **1** and **2** was investigated in the solid state at room temperature. Their emission spectra are shown in Fig. 4. Fbix exhibits an intense blue fluorescence emission band centered at 495 nm upon excitation at 336 nm. Both complexes show similar emission bands centered at *ca.* 492 and 494 nm for **1** and **2**, respectively, which can be ascribed to intraligand fluorescence emissions. It is clear from the comparison with the ligand that the Zn^{II} complexes show an enhancement of the relative emission intensity owing to ligation of the ligand to the d^{10} metal center [21, 22].

Conclusion

In summary, anion-regulated assemblies of Zn^{II} ions with the flexible fluorinated ligand Fbix lead to the formation of two new coordination polymers. Both complexes adopt different structures from a neutral chain to a cationic brick-wall network due to the difference in anion coordination. Obviously, the increase of the terminally coordinated anions leads to a reduction of the dimensionality of the coordination frameworks. The fascinating structure-function relationships of such components will promote us to make a further systematic study on the coordination chemistry of flexible *N*-containing ligands with fluorinated backbones.

Experimental Section

All reagents and solvents for synthesis were commercially available and used without further purification. Infrared spectra were recorded with a Nicolet ESP 460 Fourier transform (FT) spectrometer on KBr pellets in the range of 4000 – 400 cm^{-1}. Elemental analyses were performed with a PE2400II (Perkin-Elmer) elemental analyzer. Thermogravimetric analysis (TGA) experiments were carried on a Dupont thermal analyzer from room temperature to 800 °C (heating rate: 10 °C min^{-1}, nitrogen stream). Fluorescence spectra of the solid samples were recorded with a Varian Cary Eclipse spectrometer at room temperature.

*Synthesis of [Zn(Fbix)(OAc)$_2$]$_n$ (**1**)*

A methanol solution (15.0 mL) of Fbix (31.0 mg, 0.1 mmol) was added into a solution of $Zn(OAc)_2{\cdot}2H_2O$ (21.9 mg, 0.1 mmol) in methanol (10.0 mL). Then, the mixture was heated under reflux with stirring for *ca.* 30 min. The resulting solution was filtered and left to stand at room temperature. Colorless block-shaped crystals suitable for X-ray analysis were obtained after one week in 42 % yield (20.7 mg, on the basis of Fbix). – Anal. for $C_{18}H_{16}F_4N_4O_4Zn$ (%): calcd. C 43.79, H 3.27, N 11.35; found C 43.90, H 3.29, N 11.37. – IR (KBr pellet): $\nu = 3145$

Table 2. Crystal structure data for **1** and **2**.

	1	**2**
Empirical formula	$C_{18}H_{16}F_4N_4O_4Zn$	$C_{42}H_{36}F_{12}N_{16}O_{15}Zn_2$
M_r	493.72	1363.61
Crystal size, mm^3	$0.22 \times 0.20 \times 0.20$	$0.24 \times 0.22 \times 0.20$
Crystal system	monoclinic	triclinic
Space group	*C*2/*c*	$P\bar{1}$
a, Å	12.282(3)	9.887(1)
b, Å	12.031(3)	11.246(1)
c, Å	13.449(3)	13.870(1)
α, deg	90	109.39(1)
β, deg	99.76(1)	94.63(1)
γ, deg	90	105.81(1)
V, $Å^3$	1958.5(8)	1374.5(2)
Z	4	1
$D_{calcd.}$, g cm^{-3}	1.67	1.65
$\mu(MoK_\alpha)$, cm^{-1}	1.3	1.0
F(000), e	1000	688
hkl range	$-15 \le h \le +14$	$-11 \le h \le +11$
	$-15 \le k \le +15$	$-13 \le k \le +13$
	$-17 \le l \le +15$	$-16 \le l \le +16$
Refl. measured	6331	17 968
Refl. unique / R_{int}	2242 / 0.0764	4504 / 0.0361
Param. refined	142	406
R/R_w [a,b]	0.0423 / 0.0861	0.0489 / 0.1606
GOF (F^2) [c]	1.003	1.045
$\Delta\rho_{fin}$ (max/min), e $Å^{-3}$	0.43 / −0.66	0.96 / −0.35

[a] $R1 = \Sigma||F_o| - |F_c||/\Sigma|F_o|$; [b] $wR2 = [\Sigma w(F_o^2 - F_c^2)^2/\Sigma w(F_o^2)^2]^{1/2}$, $w = [\sigma^2(F_o^2) + (AP)^2 + BP]^{-1}$, where $P = (\mathrm{Max}(F_o^2, 0) + 2F_c^2)/3$; [c] $\mathrm{GoF} = [\Sigma w(F_o^2 - F_c^2)^2/(n_{obs} - n_{param})]^{1/2}$.

Table 3. Selected bond lengths (Å) and angles (deg) for **1** and **2** with estimated standard deviations in parentheses[a].

1		**2**	
Distances		Distances	
Zn1–O1	1.962(2)	Zn1–O1	2.009(2)
Zn1–N1	2.004(2)	Zn1–N1	2.001(2)
		Zn1–N3	1.987(2)
		Zn1–N5	1.994(2)
Angles		Angles	
O1–Zn1–O1#1	100.0(1)	O1–Zn1–N1	94.8(1)
O1–Zn1–N1	103.50(8)	O1–Zn1–N3	110.1(1)
O1–Zn1–N1#1	116.75(8)	O1–Zn1–N5	118.9(1)
N1–Zn1–N1#1	115.8(1)	N1–Zn1–N3	109.0(1)
		N1–Zn1–N5	109.0(1)
		N3–Zn1–N5	113.3(1)

[a] Symmetry code for **1**, #1: $-x+1, y+1, -z+1/2$.

(m), 2990 (w), 2980 (w), 1618 (s), 1589 (m), 1520 (m), 1490 (s), 1441 (m), 1398 (m), 1351 (m), 1328 (s), 1278 (m), 1230 (m), 1174 (w), 1115 (m), 1093 (s), 1033 (s), 1017 (m), 952 (m), 922 (w), 852 (m), 834 (m), 770 (m), 746 (m), 673 (m), 661 (s), 648 (m), 615 (w), 582 (w) cm^{-1}.

*Synthesis of {[$Zn_2(Fbix)_3(NO_3)_2$]$(NO_3)_2(H_2O)_3$}$_n$ (**2**)*

The same synthetic procedure as that described for **1** was used except that $Zn(OAc)_2 \cdot 2H_2O$ was replaced by $Zn(NO_3)_2 \cdot 6H_2O$ (29.7 mg, 0.1 mmol), giving colorless block-shaped crystals of **2** upon slow evaporation of the solvent in 65 % yield (29.5 mg, on the basis of Fbix). – Anal. for $C_{42}H_{36}F_{12}N_{16}O_{15}Zn_2$ (%): calcd. C 37.01, H 2.66, N 16.44; found C 36.81, H 2.69, N 16.57. – IR (KBr pellet): $\nu = 3446$ (bs), 3121 (m), 2995 (w), 2976 (w), 1531 (m), 1494 (s), 1457 (w), 1384 (s), 1287 (m), 1241 (w), 1112 (m), 1091 (s), 1040 (w), 944 (m), 862 (w), 768 (m), 726 (w), 657 (s), 612 (w) cm^{-1}.

X-Ray structure determinations

The single-crystal X-ray diffraction data for complexes **1** and **2** were collected on a Bruker Apex II CCD diffractometer with MoK_α radiation ($\lambda = 0.71073$ Å) at room temperature. A semiempirical absorption correction was applied (SADABS) [23], and the program SAINT was used for integration of the diffraction profiles [24]. The structures were solved by Direct Methods using SHELXS and refined by the full-matrix least-squares on F^2 using the SHELXL program [25 – 28]. All non-hydrogen atoms were refined anisotropically. Carbon-bound H atoms were placed in idealized geometrical positions and refined by using a riding model. Oxygen-bound H atoms were localized by difference Fourier maps and refined in subsequent refinement cycles. Further crystallographic details are summarized in Table 2, selected bond lengths and angles are listed in Table 3.

CCDC 1006840 and 1006841 contain the supplementary crystallographic data for this paper. These data can be obtained free of charge from The Cambridge Crystallographic Data Centre *via* www.ccdc.cam.ac.uk/data_request/cif.

Acknowledgement

We gratefully acknowledge financial support by the National Natural Science Foundation of China (21201026), the Nature Science Foundation of Jiangsu Province (BK20131142), the Open Foundation of Jiangsu Province Key Laboratory of Fine Petrochemical Technology (KF1105), and a project funded by the Priority Academic Program Development of Jiangsu Higher Education Institutions (PAPD).

[1] J. R. Li, J. Sculley, H. C. Zhou, *Chem. Rev.* **2012**, *112*, 869 – 932.
[2] M. O'Keeffe, O. M. Yaghi, *Chem. Rev.* **2012**, *112*, 675 – 702.
[3] C. Wang, T. Zhang, W. B. Lin, *Chem. Rev.* **2012**, *112*, 1084 – 1104.
[4] Y. J. Cui, Y. F. Yue, G. D. Qian, B. L. Chen, *Chem. Rev.* **2012**, *112*, 1126 – 1162.
[5] I. G. Georgiew, L. R. MacGillivray, *Chem. Soc. Rev.* **2007**, *36*, 1239 – 1248.
[6] R.-Q. Zou, C.-S. Liu, Z. Huang, T.-L. Hu, X.-H. Bu, *Cryst. Growth Des.* **2006**, *6*, 99 – 108.
[7] X. G. Meng, Y. L. Song, H. W. Hou, H. Y. Han, B. Xiao, Y. T. Fan, Y. Zhu, *Inorg. Chem.* **2004**, *43*, 3528 – 3536.
[8] B.-C. Tzeng, H.-T. Yeh, T.-Y. Chang, G.-H. Lee, *Cryst. Growth Des.* **2009**, *9*, 2552 – 2555.
[9] B. Zheng, H. Dong, J. F. Bai, Y. Z. Li, S. H. Li, M. Scheer, *J. Am. Chem. Soc.* **2008**, *130*, 7778 – 7779.
[10] X. Feng, L.-Y. Wang, J.-S. Zhao, J.-G. Wang, N. S. Weng, B. Liu, X.-G. Shi, *CrystEngComm* **2010**, *12*, 774 – 783.
[11] W. Hong, H. Lee, T. H. Noh, O.-S. Jung, *Dalton Trans.* **2013**, *42*, 11092 – 11099.
[12] E. Coronado, M. Giménez-Marqués, C. J. Gómez-García, G. M. Espallargas, *Inorg. Chem.* **2012**, *51*, 12938 – 12947.
[13] L. Carlucci, G. Ciani, S. Maggini, D. M. Proserpio, *Cryst. Growth Des.* **2008**, *8*, 162 – 165.
[14] B. F. Hoskins, R. Robson, D. A. Slizys, *J. Am. Chem. Soc.* **1997**, *119*, 2952 – 2953.
[15] L. Carlucci, G. Ciani, D. M. Proserpio, *Cryst. Growth Des.* **2005**, *5*, 37 – 39.
[16] S. R. Zheng, Q. Y. Yang, R. Yang, M. Pan, R. Cao, C. Y. Su, *Cryst. Growth Des.* **2009**, *9*, 2341 – 2353.
[17] Y. Qi, F. Luo, Y. X. Che, J. M. Zheng, *Cryst. Growth Des.* **2008**, *6*, 606 – 611.
[18] Y. Gao, B. Twamley, J. M. Shreeve, *Inorg. Chem.* **2006**, *45*, 1150 – 1155.
[19] H.-Y. Xia, X.-C. Zha, G.-X. Liu, Y. Wang, X.-M. Ren, *Chin. J. Inorg. Chem.* **2011**, *27*, 1441 – 1445.
[20] S.-C. Chen, Z.-H. Zhang, H. Xu, H.-B. Gao, R.-R. Qin, Q. Chen, M.-Y. He, M. Du, *Inorg. Chem. Commun.* **2012**, *15*, 180 – 184.
[21] A. W. Adamson, P. D. Fleischauer, *Concepts of Inorganic Photochemistry*, John Wiley & Sons, New York, **1975**.

[22] H. Yersin, A. Vogler, *Photochemistry and Photophysics of Coordination Compounds*, Springer-Verlag, Berlin, **1987**.
[23] G. M. Sheldrick, SADABS, Program for Empirical Absorption Correction of Area Detector Data, University of Göttingen, Göttingen (Germany) **2002**.
[24] SAINT, Software Reference Manual, Bruker Analytical X-ray Instruments Inc., Madison, Wisconsin (USA) **1998**.
[25] G. M. Sheldrick, SHELXTL NT (version 5.1), Bruker Analytical X-ray Instruments Inc., Madison, Wisconsin (USA) **2001**.
[26] G. M. Sheldrick, SHELXS/L-97, Programs for Crystal Structure Determination, University of Göttingen, Göttingen (Germany) **1997**.
[27] G. M. Sheldrick, *Acta Crystallogr.* **1990**, *A46*, 467 – 473.
[28] G. M. Sheldrick, *Acta Crystallogr.* **2008**, *A64*, 112 – 122.